



## Deformation analysis of a soft–hard rock contact zone surrounding a tunnel

Wenkai Feng <sup>\*</sup>, Runqiu Huang, Tianbin Li

State Key Laboratory of Geohazard Prevention and Geoenvironment Protection, Chengdu University of Technology, Chengdu, Sichuan 610059, China

### ARTICLE INFO

#### Article history:

Received 20 December 2011  
Received in revised form 10 May 2012  
Accepted 26 June 2012  
Available online 31 July 2012

#### Keywords:

Soft and hard rock contact zone  
Principal stress difference  
Principal stress ratio  
Relatively high geostress  
Large deformation mechanism  
Plastic-squeezing failure type

### ABSTRACT

The Mounigou tunnel crosses complex geological strata, mostly with surrounding rock of poor quality with an IV or V classification. Failure in the form of collapses or squeezing deformation occurred many times during the tunnel construction. Especially, in the soft and hard rock contact zone of phyllite and meta-sandstone, the deformation failure was most obvious. This paper uses the FLAC-3D modeling analytical software to establish a 3D-numerical model, on the basis of a field tracing survey and laboratory tests to analyze the stress and strain changes before and after excavation of the tunnel. After excavation there are obvious stress concentrations and differentiations near the interface of the soft-and-hard rock stratum. Stress transfers and concentrates towards the hard rock stratum while in the soft rock zone stress release could be observed to some degree. The range of plastic deformation is obviously larger in the soft rock zone than in the hard rock zone. Both differences in principal stress and principal stress ratio increase after excavation. The amplification of the difference in principal stress is larger than the augmentation of the principal stress ratio. Moreover these principal stress amplifications are smaller in the soft rock zone than in the hard rock zone. The difference in principal stress amplifications between the soft and hard rock zones, together with the fact that soft rock strength is far lower than that of hard rock, causes local “relatively high geostress” effects in the soft rock. It is the main controlling factor of the large deformation of soft rock in the tunnel. It is concluded that the large deformation in the soft and hard rock contact zone in combination with the surrounding rock deformation failure in the Mounigou tunnel and the damage of the supporting structure, belongs to the type of soft rock plastic-squeezing failure.

© 2012 Elsevier Ltd. All rights reserved.

### 1. Introduction

Large deformation of soft rock during tunnel and mine gallery excavations and underground engineering constructions is always a puzzling problem, disturbing the safety and quality of the constructions. Progress have been made in solving problems related to large deformation mechanisms of soft surrounding rock by combining engineering practice and theoretical analysis (Tan, 1982; Anagnostou, 1993; Aydan et al., 1993; Liu et al., 2005), analyzing stress and strain features of surrounding rock (Jin et al., 2004; Wang et al., 2004; Wang and Miao, 2006; Corkum and Martin, 2006; Bai et al., 2008; Zhang, 2008; Ma et al., 2008; Zhao et al., 2008; Fang et al., 2009; He et al., 2010; Huang et al., 2011; Wang, 2011), and by developing technologies for deformation prediction and forecasting (Aydan et al., 1993; Bhasin et al., 1995). Worth mentioning is also the contributions of Pelli et al. (1986), Swoboda et al. (1989), Miwa and Ogasawara (2005), Zhou (2005), Zhao et al. (2007), Liu et al. (2008), Zheng (2010), Gu (2010), Zhang et al. (2011) who developed construction methods and supporting tech-

niques to tackle the problems related to large rock deformations. However further fundamental research is needed to improve many shortcomings. For example more analyses are needed on surrounding rock stress conditions, surrounding rock structural features and the deformation continuity and expansion. Also further fundamental studies are needed about the relation between deformation features and failure and the physical-mechanical properties of soft rock and about deformation features affected by water pressure (Madsen et al., 1995). Special attention should be paid to the fact that, due to lithologic mutations such deformation failures in tunneling may occur unexpectedly as squeezing, collapsing or arch cracking (Kaiser et al., 1983; Chen et al., 2008; He et al., 2009; Wang et al., 2009; Gao et al., 2009). That will threaten the safety during the construction of the tunnel and later operations. This paper uses a 3D numerical model and its analyzing tools, to study the stress and strain features and large deformation mechanisms in the contact zone between soft rocks (mainly phyllites) and hard rocks (mainly meta-sandstones).

### 2. Basic characteristics of Mounigou tunnel

The Mounigou highway tunnel, with its total length of 1835 m and maximum embedded depth of 276 m, is the key tunnel along the important tourist route from the Songpan County downtown

\* Corresponding author. Address: College of Environment and Civil Engineering, Chengdu University of Technology, No. 1, Third East Road, Exiangqiao, Chengdu, Sichuan 610059, China. Tel./fax: +86 2884073193.

E-mail address: fengwenkai@cdut.cn (W. Feng).

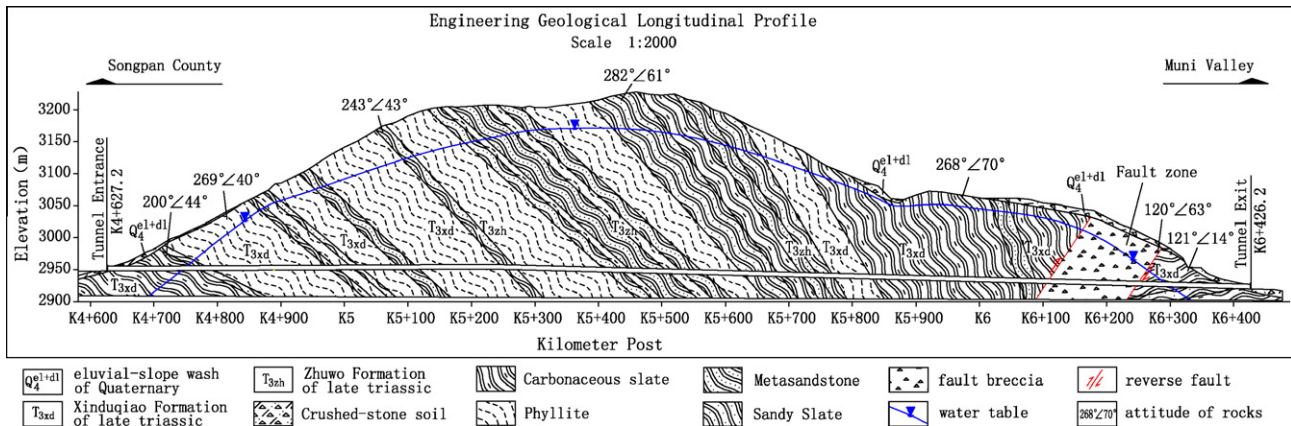


Fig. 1. Cross-section of the tunnel strata.

area to the Mounigou Scenic spot. The tunnel is located in the mountainous area west of the Mingiang River and to the east of Mounigou. The landform is characterized by middle and high mountain erosion features and tectonic denudation, with quite complex geological structures, strongly influenced by tectonism.

Detailed field investigations revealed that the entrance and exit area of the tunnel goes through quaternary gravelly soil layers while the main part of the tunnel will cross phyllitic rocks carbonaceous slates, sandy slates, with interlayers of meta-sandstones. It will also pass a fault fracture zone, belonging to Zhuwo and Xinduqiao formations of the Late Triassic. Among those, the slightly weathered phyllites and carbonaceous slates are soft to extremely soft rocks whereas the slightly weathered meta-sandstone and sandy slates are relatively hard rocks. On the whole, the surrounding rock is of poor quality. The thickness of the mono-layered strata is relatively thin and strongly influenced by regional tectonic activity. There is well-developed secondary fold and fault zones and interlayer fracture zones, which gives the whole rock body a broken and spongy character, with well-developed joints, rich of ground water. Because of these complex structures and weak character these surrounding rocks are classified, mainly as IV and V. Fig. 1 shows the strata along the cross-section of the tunnel.

Because of the above mentioned complex and poor geological conditions in the tunnel setting, chip off-falling in collapse, exfoliation, and local arch slumping occurred regularly during the construction. Once, a lump arch of 5 m high jammed the tunnel and brought about serious safety problems (shown in Fig. 2). For example, on July 31st, 2010, at 12 p.m. a serious tunnel collapse occurred in the K5+060–K5+067 entrance section. The estimated volume of the collapsed material is around 500 m<sup>3</sup>, with a height 5–6 m, and a width 12 m (Fig. 2b). It happened because of the poor lithology which consists of carboniferous sericitic and phyllitic rocks, with well-developed secondary joints filled with calcites and intrusions of quartzitic dikes. Similar failures most obviously occurred also in soft-and-hard rock contact zones. Local chip off-falling can occur in the hard rock area due to a strong deformation of the soft rock.

### 3. 3-D numerical modeling analysis

The FLAC-3D modeling analytical software was used, developed by American ITASCA Company which examined the stress and strain features in the contact area of phyllites and meta-sandstones before and after the excavation. It builds a solid foundation for better understanding deformation failure phenomena and mechanisms in the soft-and-hard rock contact area.



(a) Over excavation formed by local arch collapse



(b) serious collapse in K5+060~K5+067 section

Fig. 2. Tunnel deformational failure phenomenon.

#### 3.1. Model generalization and parameter determination

Considering of the factors as 3-D modeling complexity, calculation efficiency and research optimization, the soft-and-hard rock contact area with largest embedded depth (pile No. K5+140), was chosen for the research. A model frame 250 m long and 250 m wide was established and the model is bounded by a zone of 100 m above

and 100 m below the tunnel (What needs to be explained is that, the thickness of the upper rocks in here is about 250 m. In order to simplify the modeling process and to reduce the amount of simulation computing, it was valued as 100 m in the modeling process. But during the calculation, another amount of 150 m upper rock's self-weight stress was imposed.). It consists of two materials, soft phyllite and hard meta-sandstone. The network consists of 29996 nodal points and 175533 units (see Fig. 3). Material parameters were mainly determined through field tests. It adopts analogical synthesized sampling, with reference to concerned codes (shown in Table 1). The elastic-plastic constitutive model and Mohr-Coulomb yield criterion were used in the simulations and analyses.

### 3.2. Modeling results analysis

#### 3.2.1. Stress field features of surrounding rock before tunnel excavation

The calculated result of the surrounding rock stress field before the tunnel excavation is shown in Figs. 4 and 5. The calculated maximum and minimum principal stress distribution before the excavation reveal that:

- (1) The surrounding rock within the periphery of the cavity is controlled by self-weight stress, showing an regular increase in stress with depth without obvious differentiations and mutations.
- (2) In the soft-and-hard rock contact zone, the maximum principal stress of the surrounding rock within the periphery of the cavity is about 7.9 MPa, while the minimum is about 3.0 MPa.

- (3) In the horizontal direction, which is bounded by the lithologic interface, the stress difference between the two sidewalls is quite small. At the same elevation the stress in the phyllite section is a bit smaller than that in meta-sandstone section with differences ranging between 0.2 MPa and 0.4 MPa.

#### 3.2.2. Stress field features of surrounding rock after tunnel excavation

Stress and yield of deep-buried surrounding rock, on the periphery of the cavity, after excavation, are shown in Fig. 6 until Fig. 9. The calculation results reveal:

- (1) There is great change of the stress state in the surrounding rock within the periphery of the cavity. Stress increases obviously, and the maximum principal stress concentrates on the sidewalls and top arch, with measured values larger than 12 MPa.
- (2) The rock of the left sidewall and base plate consist of phyllites while the right sidewall and top arch consist of meta-sandstones, and the stress levels of those areas vary distinctly. Fig. 6a shows that the maximum principal stress on the right sidewall is larger than on the left sidewall, and the stress peak value in the top arch is larger than in the base plate. Similar distributions show the minimum principal stresses (see Fig. 7). Before and after excavation, maximum and minimum principal stresses concentrate on the tunnel walls as shown in Table 2. The amplification of the maximum and minimum principal stress in the meta-sandstone zone surrounding the top arch and the right

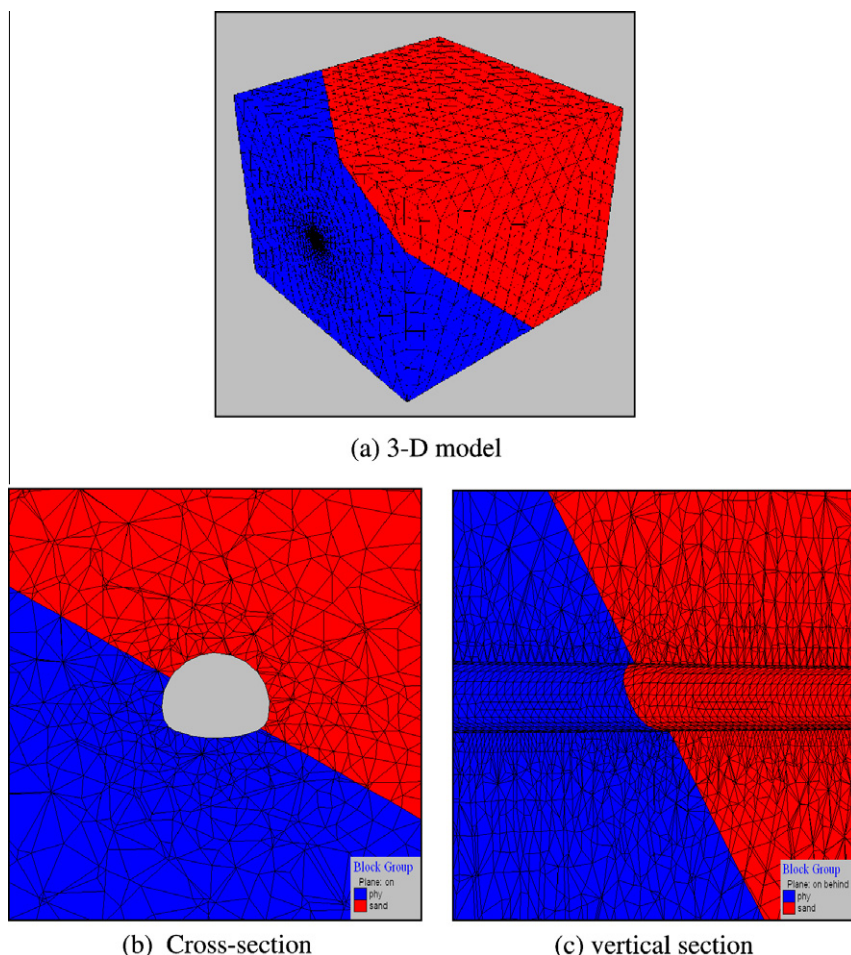
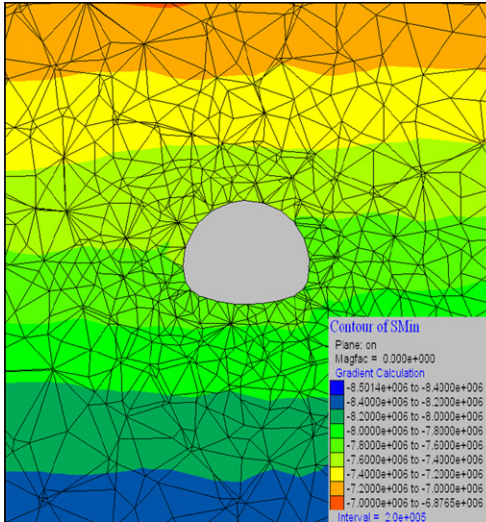


**Fig. 3.** Model material segmentation and grid division (blue part on the lower left side represents phyllite; red part on the upper right represents meta-sandstone). (For interpretation of the references to color in this figure legend, the reader is referred to the web version of this article.)

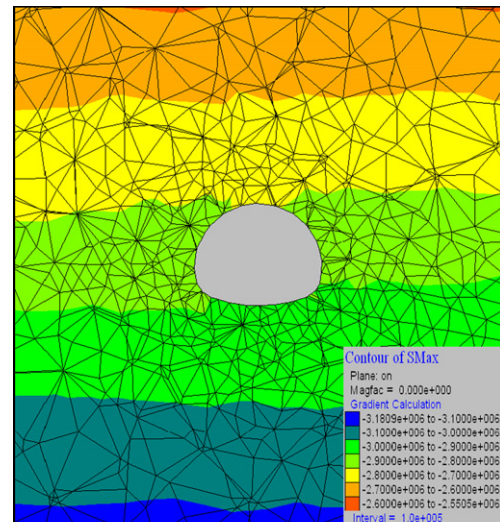
**Table 1**

Numerical modeling parameter determination.

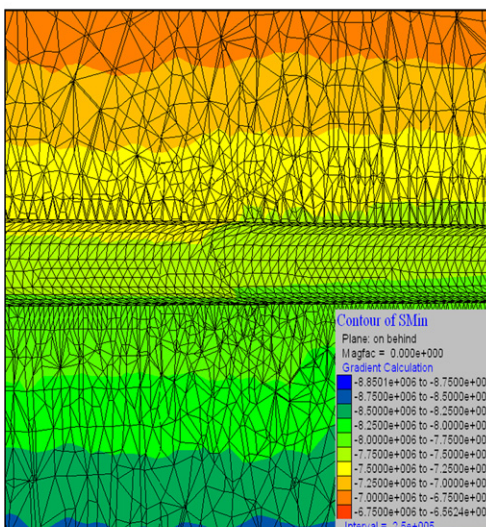
	Volume weight ( $\text{kg}/\text{m}^3$ )	Elastic modulus (GPa)	Poisson's ratio, $\mu$	Cohesion force (MPa)	Internal friction angle ( $^\circ$ )	Tensile strength (MPa)
Meta-sandstone	2630	9	0.29	3.0	35	1.0
Phyllite	2620	3	0.30	1.7	30	0.4
Joint plane				0.7	30	



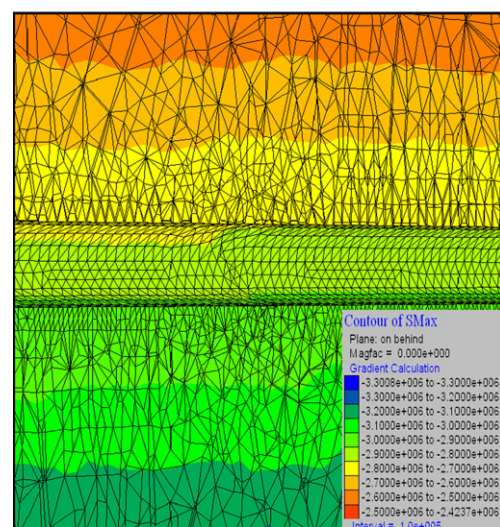
(a) horizontal distribution



(a) horizontal distribution



(b) vertical distribution



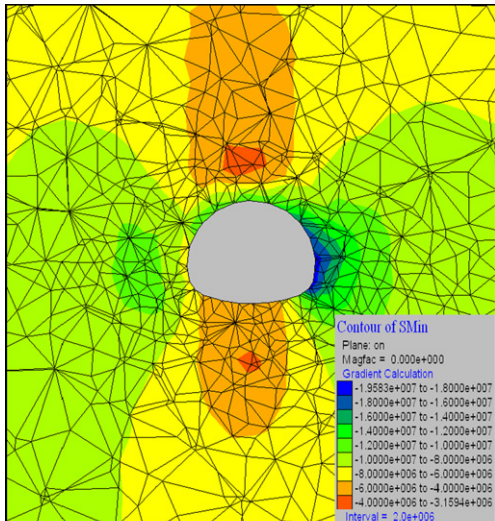
(b) vertical distribution

**Fig. 4.** Distribution diagram of the tunnel-surrounding rock's maximum principal stress before excavation (the tunnel materials are hidden in the diagram).**Fig. 5.** Distribution diagram of tunnel surrounding rock's minimum principal stress before excavation (the tunnel materials are hidden in the diagram).

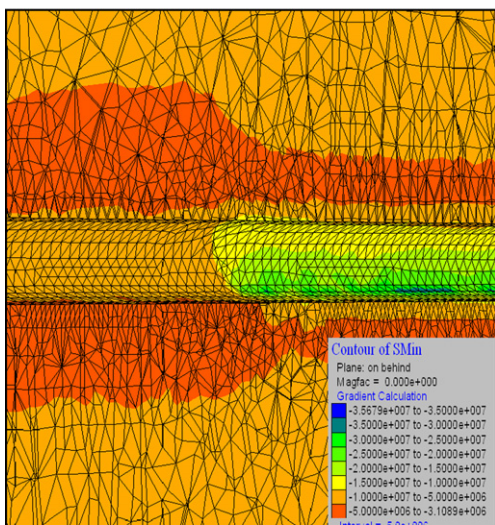
sidewall of the tunnel is larger than in the phyllitic zone of the base plate and the left sidewall. On the whole, the maximum principal stresses on the tunnel walls are 2.41 times larger than before the excavation, and the minimum principal stresses increased 1.38 times. The maximum amplification factor of the principal stress difference is 3.0, and the minimum amplification factor of the principal stress ratio is 2.06. It creates favorable conditions for rock failure. This can be demonstrated by plotting the Mohr-circle diagrams of the principal stresses of the top arch and right sidewall before and after the excavation (see Fig. 8). The Figure shows

that, before excavation, the stress level of the surrounding rock does not reach the shear strength envelope of the rock and their joint planes. But after excavation, the stress concentration levels surpass the shear strength envelope of the phyllites and their joint planes, which indicates rock failure.

(3) Along the length of tunnel, after excavation the maximum principal stress of the meta-sandstone near the phyllitic zone is 7–15 MPa larger than that of phyllitic rock. In this section the meta-sandstone not only adapts to the stress changes caused by the excavation itself but also for a part to the



(a) horizontal distribution

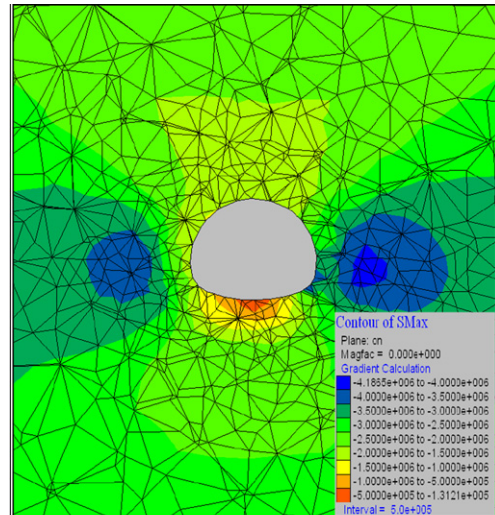


(b) vertical distribution

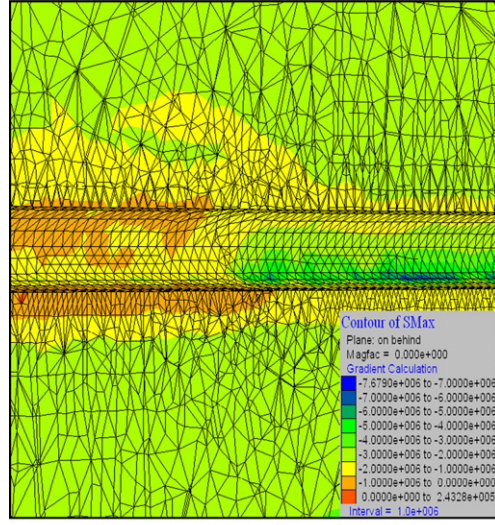
**Fig. 6.** Distribution diagram of tunnel surrounding rock's maximum principal stress after excavation.

stress and strain caused by phyllitic rock excavation. Therefore, the closer to the phyllitic rock zone, the higher the stress values of the meta-sandstone zone. According to calculations, the estimated distance where the phyllitic zone influences the stress values of the meta-sandstone lies between 15 and 25 m. The hard rock in the soft-and-hard rock contact zone exhibits a stress concentration area. In case of a fine layered sandstone formation with a relative small thickness attention should be paid to the construction of that part of the tunnel. Meanwhile, a stress concentration to some degree on the hard rock section, indicates that there exists a relatively large stress release area in the soft rock part of the contact zone (shown in Fig. 7) causing a small increase in the plastic deformation and its distribution area (shown in Fig. 9).

- (4) Because of the difference in lithology between two lateral tunnel sides, peak stress values are not evenly distributed. On the right tunnel side, the peak value of the principal stresses appeared outside of the tunnel wall, while on the left side, the peak values appeared in internal depth away



(a) horizontal distribution



(b) vertical distribution

**Fig. 7.** Distribution diagram of tunnel surrounding rock's minimum principal stress after excavation.

from tunnel wall. The stress distribution is closely related to the type of material. Meta-sandstone has higher strength and mechanical properties than phyllite's and therefore the rock body can bear relatively strong stresses without failure while phyllites cannot bear intense stress change after excavation and failure occurs. The immediate surrounding rock loses strength and the deep-seated surrounding rock needs to bear these stress changes triggered by the tunnel excavation. There appears some stress concentration at the top arch and base plate of the tunnel, away from the tunnel walls, which indicates that obvious failure occurs as is shown in Fig. 9a.

- (5) The distribution map of the plastic deformation area (Fig. 9) shows that yielding mainly occurs within the range of tunnel top arch and its invert. The Plastic deformation area of the two lateral tunnel wall sides has an average width of 3 m. The deformation area of the top plate has a range of 10–11 m in the phyllite stratum, and 7–8 m in the sandstone stratum. The Yielding area of the base plate has the trend to extend along two sides of the tunnel. The plastic deforma-

**Table 2**

Contrastive analysis of stress concentration in tunnel wall before and after excavation.

Wall part	Before excavation				After excavation				Amplification of principal stress ratio $(\sigma'_1/\sigma'_3)/(\sigma_1/\sigma_3)$	Amplification of principal stress difference $(\sigma'_1 - \sigma'_3)/(\sigma_1 - \sigma_3)$
	$\sigma_1$	$\sigma_3$	$\sigma_1/\sigma_3$	$\sigma_1 - \sigma_3$	$\sigma'_1$	$\sigma'_3$	$\sigma'_1/\sigma'_3$	$\sigma'_1 - \sigma'_3$		
Left sidewall	7.8	2.9	2.69	4.9	8.0	2.0	4.0	6.0	1.49	1.22
Right sidewall	7.9	2.9	2.72	5.0	19.0	4.0	4.75	15.0	1.74	3.00
Top arch	7.6	2.8	2.71	4.8	14.0	2.5	5.6	11.5	2.06	2.40
Base plate	7.8	3.0	2.60	4.8	4.5	1.2	3.75	3.3	1.44	0.69

Notes:  $\sigma_1, \sigma'_1$  represents maximum principal stress before and after excavation respectively;  $\sigma_3, \sigma'_3$  represents minimum principal stress before and after excavation respectively; Stress unit: MPa.

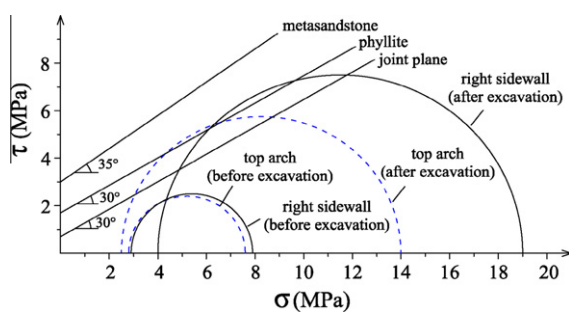


Fig. 8. The Mohr-circle diagram of shear strength before and after excavation.

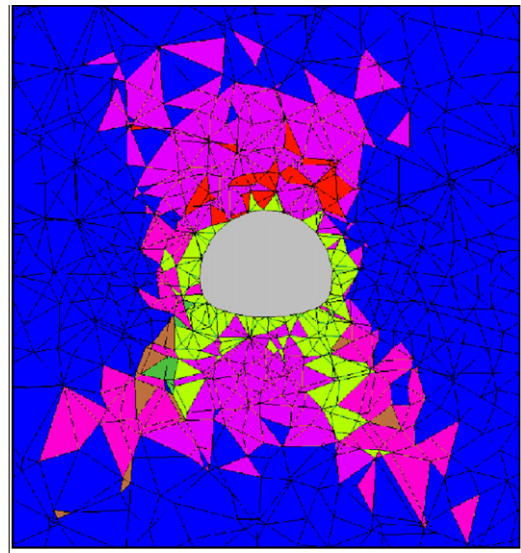
tion area in phyllites is 15 m while the yielding area in sandstones varies generally between 8 and 10 m. On the whole, the yielding area of the base plate is obviously larger than that of the top plate.

### 3.2.3. Strain field features of the surrounding rock after tunnel excavation

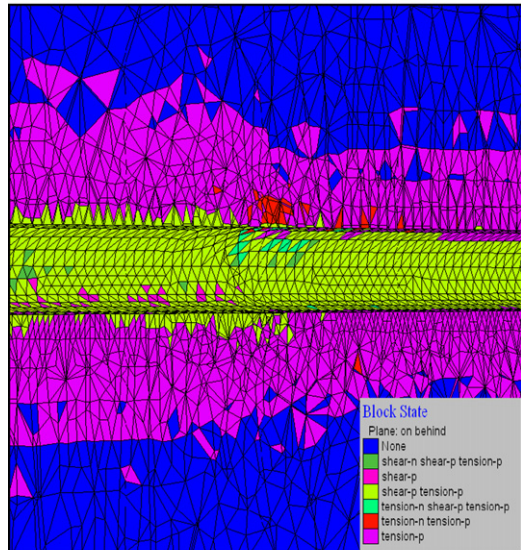
Fig. 10 shows the distribution trend of the global displacement of surrounding rock after excavation. Deformation mainly occurs near the base plate and the left lateral tunnel wall (on the phyllite side). It is predominantly radial deformation toward the tunnel center. The peak deformation value near the base plate reaches 21 cm, while on the left sidewall it amounts to 12 cm. Deformation values in the meta-sandstone zone are obviously lower than in phyllitic zone, except for a part of the meta-sandstone zone near the phyllitic zone.

## 4. Analysis of large deformation mechanism of surrounding rock

Combining modeling analysis of stress-strain features in tunnel soft-and-hard rock contact zones with actual field geological conditions and large deformation phenomena in engineering constructions, it is concluded that because of the impact by secondary stress adjustment after excavation, soft-and-hard rock stress differences will change and stress concentration will transfer toward the hard rock area. The mechanism of large rock deformation belongs to the type of soft rock plastic-squeezing failure. Due to the great stress difference in the surrounding rock formed after excavation together with the influence of underground water, the soft surrounding rock is slowly squeezed out and plastic flow occurred, which caused large deformations. The most typical example can be found at the phyllite and meta-sandstone contact zone in the K6+305–K6+365 section near the exit of the tunnel. The fractured phyllite layers with white calcites fillings in fissure deformed violently and strong plastic failure occurs: the tunnel top arch subsides for 150–300 mm, even until 358 mm and the periphery convergence amounts to 30–45 mm. The large deformation of the

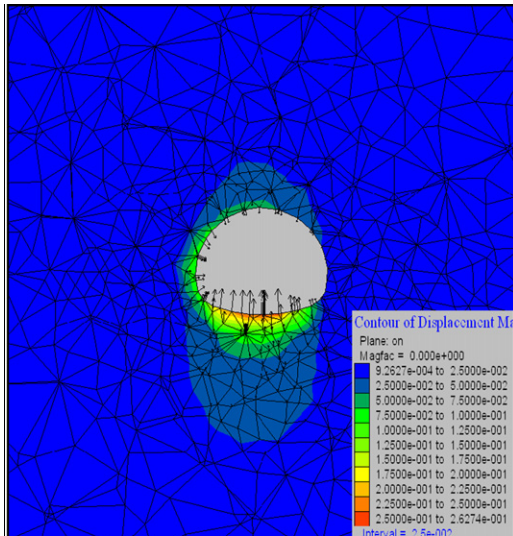


(a) horizontal distribution

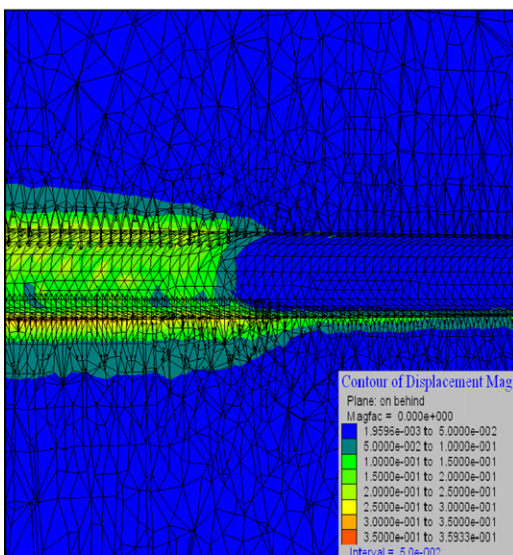


(b) vertical distribution

Fig. 9. Distribution diagram of yielding units after excavation. (Block State additional remarks: 'None' represents not yield; 'shear-n shear-p tension-p' represents the current shear stress is more than the yield strength, and shear and tension damage has happened; 'shear-p' represents shear failure has ever happened, yet the current shear stress is not more than the yield strength; 'shear-p tension-p' represents shear and tension failure have ever happened, yet the current shear and tension stress are not more than the yield strength; 'Tension-n shear-p tension-p' represents shear and tension failure have ever happened, and the current tension stress is more than the yield strength; 'Tension-n tension-p' represents tension failure has happened, and the current tension stress is more than the yield strength; 'tension-p' represents tension failure has happened, yet the current tension stress is not more than the yield strength.)



(a) horizontal distribution



(b) vertical distribution

**Fig. 10.** Distribution diagram of global displacement after excavation.

surrounding rock causes cracking, delamination, and obscession of initial supporting jet concrete, even squeezes out multi-arch flange beams leading to the deformation shown in Fig. 11a. Meanwhile, in the hard rock area, there appears strong additional deformation and line cracking (Fig. 11b).

Combined with the above case, it needs to be emphasized that the burial depth of the tunnel vault is only around 100 m in the section, and the maximum surrounding rock stress is only 2.7 MPa. Generally, large deformations may not happen at this stress level generally, but in fact it occurred. This shows that, after tunnel excavation, the stress ratio and especially the stress difference greatly increased which led to a relatively high stress transition of the surrounding rock. It should be noted that there is a diversity in grow of the soft and hard rock stress ratio and stress difference and that the soft rock strength is far lower than the hard rock strength. Therefore the weak rock area first reached its large deformation limits even under the action of a relatively low geo-stress. The large deformation in the soft rock was the main controlling factor in the hard and soft rock contact zone.



(a) large deformation in K6 + 363 ~ K6 + 367 section



(b) local cracking of initial supporting

**Fig. 11.** Initial supporting failure caused by surrounding rock large deformation.

## 5. Conclusion

According to the above analysis, the following conclusions can be made:

- (1) Before excavation, the stress of the surrounding rock on the periphery of the cavity is controlled by self-weight stress, which shows the trend of a terrace increase in depth, without clear differentiations and mutations. There is a little stress distribution mutation on the oblique plane of the soft-and-hard rock contact zone, mainly caused by stress value differences between the soft rock and hard rock zone.
- (2) After excavation there are clear stress concentrations and differentiations because of lithologic differences around the tunnel wall perimeter. The degree of stress concentration in the hard rock zone is obviously larger than in the soft rock zone. The difference in principal stresses, after excavation increases 3.0 times and principal stress ratio 2.06 times, which provide favorable stress setting conditions
- (3) There exists a clear increase in the stress concentration area both in the soft and hard rock zone. It indicates that stress near the contact zone concentrates toward the hard rock formation. It also shows that there is an increasing stress release area in the soft rock zone and that plastic deformation and its distribution area increase. The analysis shows that the stress difference amplification in the contact zone, together with the lower strength of the soft rock, causes locally a relatively high ground stress in the periphery of the soft rock area, which becomes the predominant controlling factor of the large deformation in soft rock.

(4) Stress development and its distribution in the soft and hard rock zone explain rather well the deformational failure phenomenon observed during the construction of Mounigou tunnel. The large deformation mechanism in the soft and hard rock contact zone belongs to the soft rock plastic-squeezing failure type.

## Acknowledgment

The research project is supported by The National Natural Science Foundation of China (Grant Number: 41172278) and by The Cultivating Programme of Excellent Innovation Team of Chengdu University of Technology (Grant Number: HY0084). The authors like to express their gratitude to all concerned people and authorities for the help offered in this research. They gratefully acknowledge the assistance from Doctor Li Guo, Master Liu Jintao and Guo Zhen in indoor data processing. Thanks should also go to lecturer Qiuqun Qiao from the Chengdu University of Technology and professor Theo van Asch from the Utrecht University, Netherlands for their help with the English translation.

## References

- Anagnostou, G., 1993. A model for swelling rock in tunneling. *Rock Mechanics and Rock Engineering* 26 (4), 307–331.
- Aydan, O., Akagi, T., Kawamoto, T., 1993. The squeezing potential of rocks around tunnels: theory and prediction. *Rock Mechanics and Rock Engineering* 26 (2), 137–163.
- Bai, S.W., Han, C.R., Gu, Y.L., et al., 2008. Research on crustal stress measurement and inversion of stress disturbed area of a tunnel. *Rock and Soil Mechanics* 29 (11), 2887–2892.
- Bhasin, R., Barton, N., Grimstad, E., et al., 1995. Engineering geological characterization of low strength anisotropic rocks in the Himalayan region for assessment of tunnel support. *Engineering Geology* 40 (3–4), 169–193.
- Chen, Z.H., Wang, W.Q., Zhang, L.W., 2008. FEM analyses of stress and deformation of a flexible inner pressure bolt. *Journal of China University of Mining and Technology* 18 (4), 584–587.
- Corkum, A.G., Martin, C.D., 2006. The mechanical behavior of weak mudstone (Opalinus Clay) at low stresses. *International Journal of Rock Mechanics and Mining Sciences* (4), 4–15.
- Fang, J.Q., Hu, J.Y., Lin, C.K., et al., 2009. Analysis on geo-stress evolution and construction mechanics of fault zone for Chalinding Tunnel. *Chinese Journal of Underground Space and Engineering* 5 (3), 536–540.
- Gao, M.S., Dou, L.M., Xie, Y.S., et al., 2009. Latest progress on study of stability control of roadway surrounding rocks subjected to rock burst. In: Proceedings of the 6th International Conference on Mining Science and Technology. Leiden. Procedia Earth and Planetary Science, pp. 409–413.
- Gu, P., 2010. The influence of floor heaving to deep soft rock deformation and control measures. *Journal of North China Institute of Science and Technology* 7 (2), 23–25.
- He, M.C., Gong, W.L., Li, D.J., et al., 2009. Physical modeling of failure process of the excavation in horizontal strata based on IR thermography. *Mining Science and Technology* 19 (6), 689–698.
- He, M.C., Guo, H.Y., Chen, X., et al., 2010. Numerical simulation analysis of large deformation of deep soft rock engineering based on solar decomposition theorem. *Chinese Journal of Rock Mechanics and Engineering* 29 (Supp. 2), 4050–4055.
- Huang, K., Peng, J.G., Liu, B.C., et al., 2011. Analysis of initial rock stress field and secondary rock stress field of Xuefengshan tunnel. *Journal of Central South University (Science and Technology)* 42 (5), 1454–1460.
- Jin, X.G., Li, X.H., Ai, J.R., et al., 2004. Numerical modeling of in-situ stress and surrounding rock displacement of deep-long tunnel. *Hydrogeology and Engineering Geology* 1, 40–43.
- Kaiser, P.K., Maloney, S., Morgenstern, N.R., 1983. The time dependent properties of tunnel in highly stressed rocks. In: Proceedings of the 5th Congress ISRM (D). [s. l.]:A.A. Balkema, pp. 329–335.
- Liu, G., Zhang, F.Y., Li, X.Z., et al., 2005. Research on large deformation and its mechanism of muzhailing tunnel. *Chinese Journal of Rock Mechanics and Engineering* 24 (Suppl. 2), 5521–5526.
- Liu, Z.C., Li, W.J., Zhu, Y.Q., et al., 2008. Research on construction time of secondary lining in soft rock of large-deformation tunnel. *Chinese Journal of Rock Mechanics and Engineering* 27 (3), 580–588.
- Ma, K., Xu, J., Zhang, Z.L., et al., 2008. The back analysis method based on practical secondary-stress value on its application to engineering. *Journal of Sichuan University: Engineering Science Edition* 40 (6), 51–56.
- Madsen, F.T., Fluckiger, A., Hauber, L., et al., 1995. New investigation on swelling rocks in the Belchen Tunnel, Switzerland. In: Proceedings of the 8th ISRM Congress [s. l.]: A.A. Balkema, pp. 263–267.
- Miwa, M., Ogasawara, M., 2005. Tunneling through an embankment using an all ground fasten method. *Tunneling and Underground, Space Technology* 20 (2), 121–127.
- Pelli, F., Kaiser, P.K., Morgenstern, N.R., 1986. Three-dimensional simulation of rock liner interaction near Tunnel face. In: Proceedings of the 2nd International Symposium on Numerical Models in Geomechanics, Ghent:[s. n.], pp. 359–368.
- Swoboda, G., Mertz, W., Schmid, A., 1989. Three-dimensional numerical model to simulate tunnel excavation. In: Proceedings of the 3rd International Conference on Numerical Models in Geomechanics, Niagara Falls: [s. n.], pp. 536–548.
- Tan, T., 1982. The mechanical problems for the long-term stability of underground galleries. *Chinese Journal of Rock Mechanics and Engineering* 1 (1), 1–19.
- Wang, J.J., 2011. Deformation mechanisms and classification of soft rock mass of tunnels in high ground stress zones: case study on tunnels on Lanzhou-Chongqing railway. *Tunnel Construction* 31 (3), 289–293.
- Wang, L.G., Miao, X.X., 2006. Numerical simulation of coal floor fault activation influenced by mining. *Journal of China University of Mining and Technology* 16 (4), 385–388.
- Wang, W., Wang, L.J., Qiao, Z.J., et al., 2004. Modeling of three dimensional crustal stress field and its application in tunnel design. *Acta Geoscientia Sinica* 25 (5), 587–659.
- Wang, J.X., Lin, M.Y., Tian, D.X., et al., 2009. Deformation characteristics of surrounding rock of broken and soft rock roadway. *Mining Science and Technology* 19 (2), 205–209.
- Zhang, J.H., 2008. Construction Mechanical behavior analysis on baozhen tunnel in soft rock strata with high geostress. *Subgrade Engineering* 4, 78–79.
- Zhang, W.X., Sun, S.F., Liu, H., 2011. Construction techniques of Muzhailing tunnel with high ground stresses and large soft rock deformations. *Modern Tunnelling Technology* 48 (2), 78–82.
- Zhao, X.F., Wang, C.M., Kong, X.L., 2007. Analysis of time-space effects of construction behavior of deep soft rock tunnel. *Chinese Journal of Rock Mechanics and Engineering* 26 (2), 404–409.
- Zhao, Y.T., Fan, B., Liang, H., et al., 2008. Determination of initial earth Stress of large deeply-buried tunnel. *Chinese Journal of Underground Space and Engineering* 4 (1), 147–151.
- Zheng, J.S., 2010. Discussion on construction technology of highway tunnel through the fault and fracture zone for highway. *Soil Engineering and Foundation* 24 (2), 17–19.
- Zhou, S.H., 2005. Principles of pipe roof applied to shallow-buried tunnels in soft ground. *Chinese Journal of Rock Mechanics and Engineering* 24 (14), 2565–2570.